



Supplement of

Extraction of multiple ages from *c*-axis projected fission tracks

Peter K. Jensen

Correspondence to: Peter K. Jensen (pklje@dtu.dk)

The copyright of individual parts of the supplement might differ from the article licence.

Calculated age nodes based on fission track data from the Canadian Shield (Spiegel et al., 2023b;2023b) is given in Table S1. The deconvolved fission track length histograms are shown in Fig. S1-S25.

Table S1. Calculated age nodes related to deconvolved track length (this study). Rock age is based on stratigraphy given by (Spiegel et al., 2023a) and Geologic Time Scale v. 6.0 (The Geological Society of America). Oldest age (this study), Central age (Spiegel et al., 2023a).

Sample Lithology	Rock age	Deconvolved track length	Age nodes	Calibration factor
	Oldest age Central age			
	Ma	µm	Ma	
C-XI-119 Sandstone	388-393	13	222 (52)	1.22
	461 (42)	12	427 (69)	
	318 (26)			
C-XI-120 Sandstone	388-393	13	176 (76)	1.15
	560 (62)	12	558 (81)	
	387 (42)			
C-XI-121 Granite	1600-2500	13	250 (82)	1.15
	510 (60)			
	321 (31)			
C-XI-123 Granite	1600-2500	12	410 (62)	1.16
	464 (57)			
	285 (29)			

C-XI-124 Sandstone	388-393	13	201 (31)	1.16
	322 (24)	12	322 (25)	
	236 (108)			
C-XI-125 Sandstone	383-393	13	198 (34)	1.08
	289 (22)	12	290 (22)	
	212 (14)			
C-XI-126 Sandstone	359-383	13	164 (92)	1.07
	458 (57)	11	458 (57)	
	265 (22)			
CXII-06 Sandstone	247-252	12	307 (69)	1.22
	344 (68)			
	218 (28)			
CXII-13 Granite	1600-2500	13	150 (24)	1.06
	214 (17)	12	214 (17)	
	160 (11)			
CXII-14 Granite	1600-2500	13	109 (44)	1.3
	339 (27)	12	338 (47)	
	235 (18)			
CXII-20 Sandstone	383-393	13	442 (178)	1.3
	730 (230)			
	533 (151)			
CXII-22 Sandstone	359-383	13	228(19)	1.13
	523 (95)	12	619 (87)	
	399 (36)			
CXII-25 Migmatite	1600-2500	13	153 (41)	1.05
	504 (122)	12	350 (55)	
	288 (24)			
CXII-27 Sandstone	388-393	13	265 (55)	1.38
	477 (40)	12	436 (59)	
	330 (27)			
CXII-30 Sandstone	56-59	13	257 (74)	1.5
	507 (44)	12	507 (44)	
	363 (30)			

CXII-36 Orthogneiss	1600-2500	13	377 (106)	1.43
	739 (101)	12	739 (101)	
	530 (66)			
CXII-37 Pyroxenite	1600-2500	13	273 (94)	1.21
	661 (151)			
	423 (54)			
CXII-42 Sandstone	388-393	13	183 (37)	1.26
	431 (57)	12	357 (61)	
	280 (22)			
CXII-46 Sandstone	359-383	14	82(10)	1.66
	521 (77)	13	316 (31)	
	386 (28)	12	518 (58)	
CXII-48 Sandstone	388-393	13	420 (83)	1.61
	528 (62)			
	373 (37)			
GRÖ21 Gneiss	2500-4000	13	67 (20)	1.02
	173 (25)	11	173 (25)	
	99 (9)			
GRÖ23 Sandstone	541-2500	13	136 (23)	1.07
	223 (22)	12	223 (22)	
	162 (16)			
GRÖ36 Schist	2500-4000	13	100 (36)	0.931
	204 (32)	12	204 (32)	
	146 (20)			
GRÖ64 Gneiss	2500-4000	13	138 (42)	1.004
	315 (47)	11	315 (47)	
	160 (11)			
KP702 Granite	1600-2500	13	421 (84)	1.34
	838 (171)	12	756 (138)	
	583 (69)			

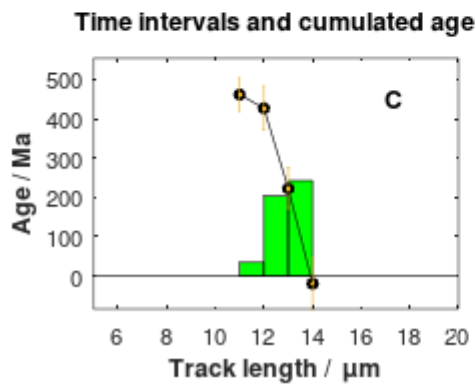
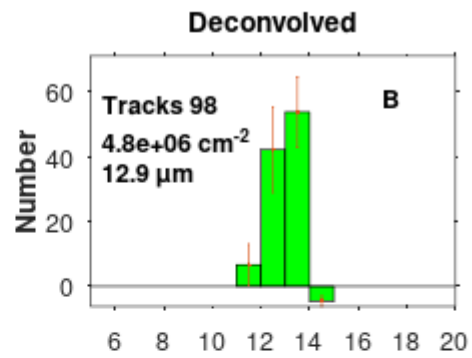
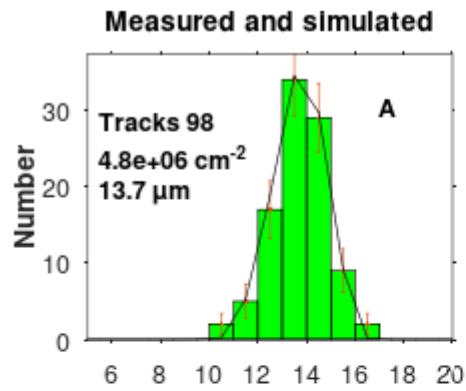


Fig. S1. C-XI-119.

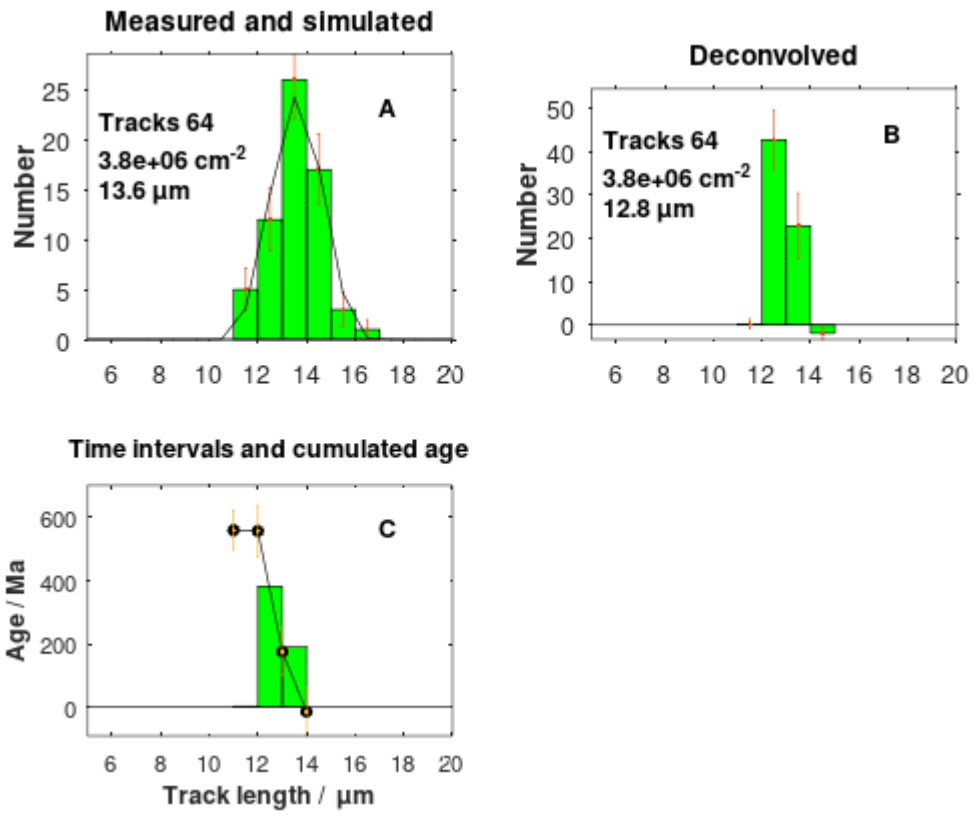


Fig. S2. C-XI-120.

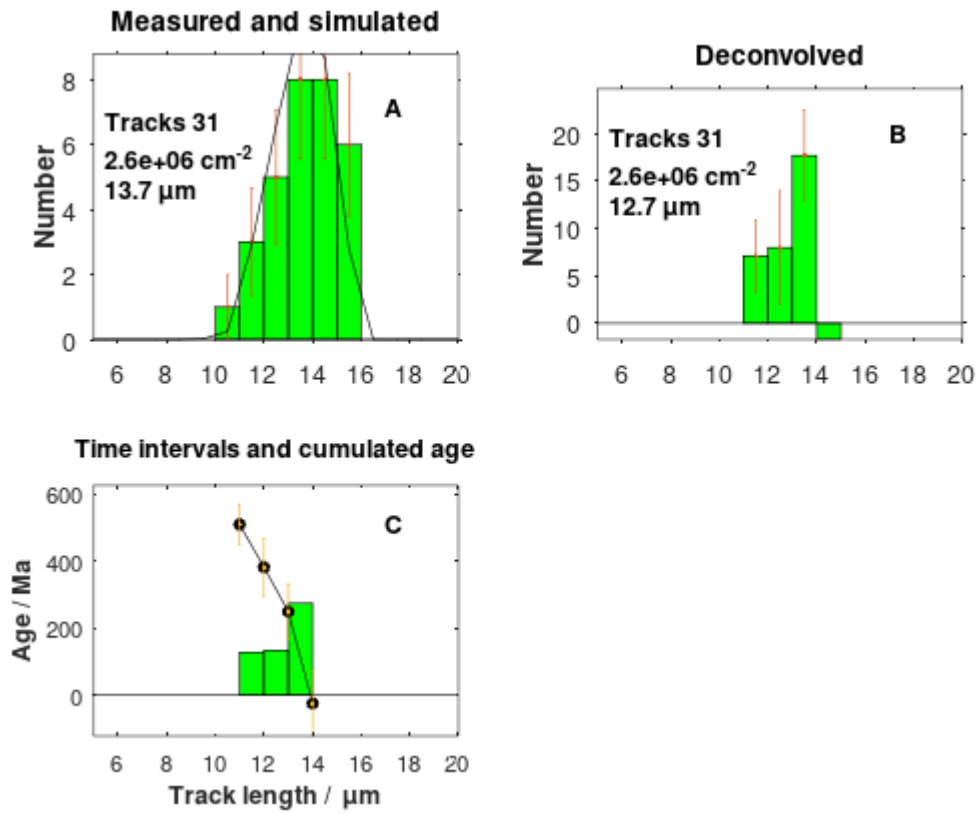


Fig. S3. C-XI-121.

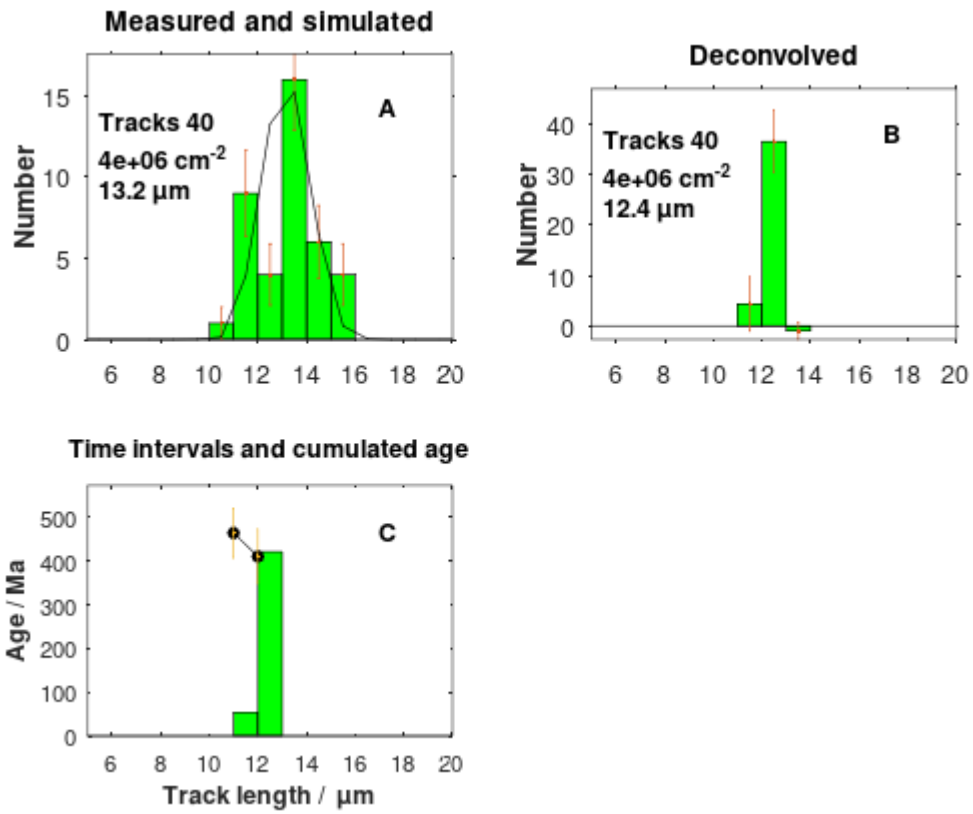


Fig. S4. C-XI-123.

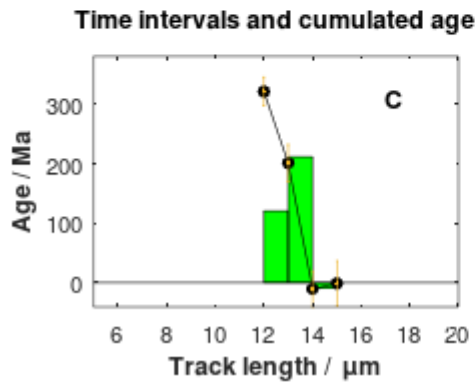
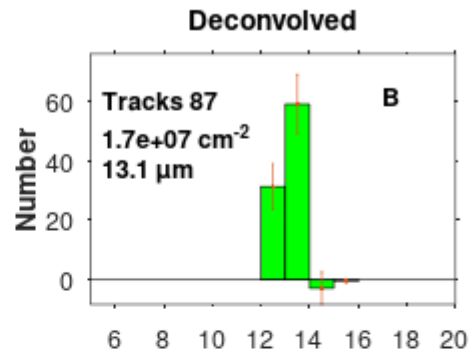
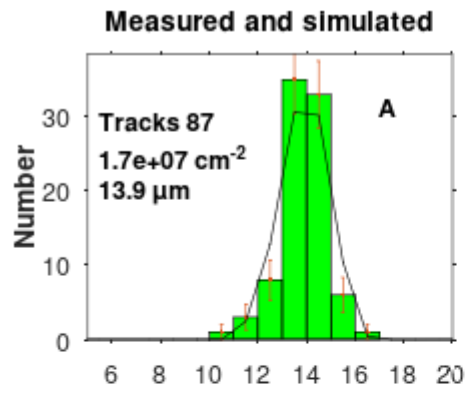


Fig. S5. C-XI-124.

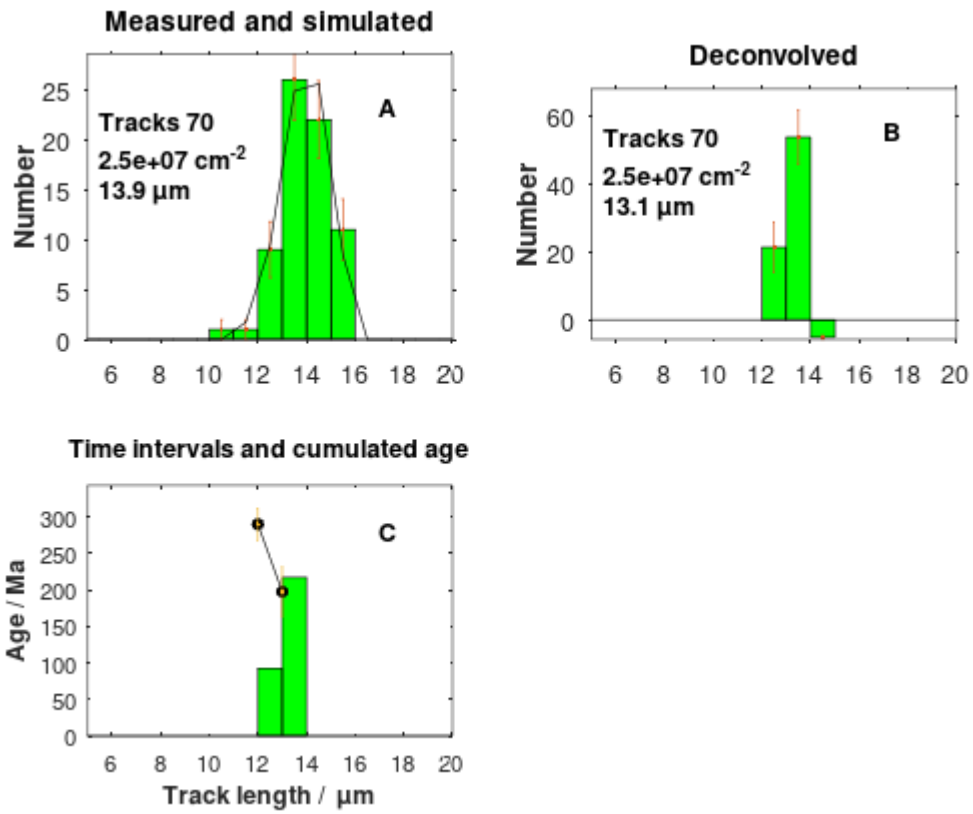


Fig. S6. C-XI-125.

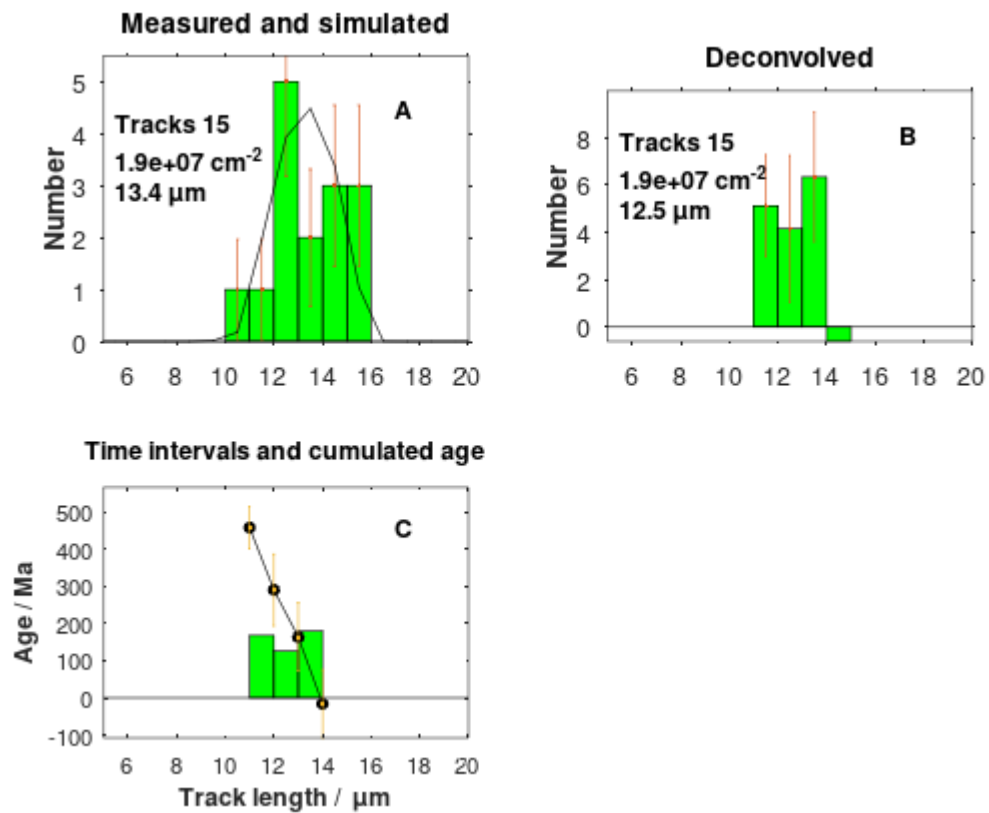


Fig. S7. C-XI-126.

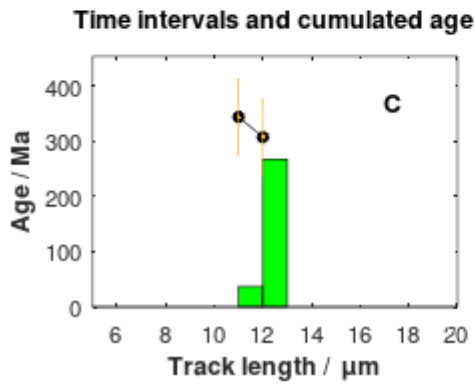
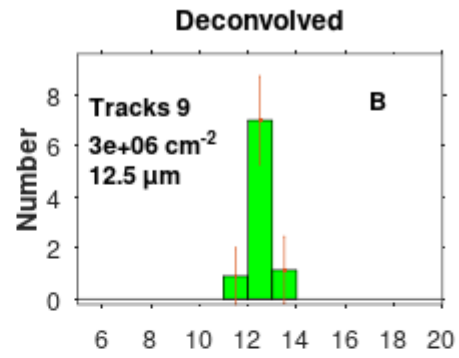
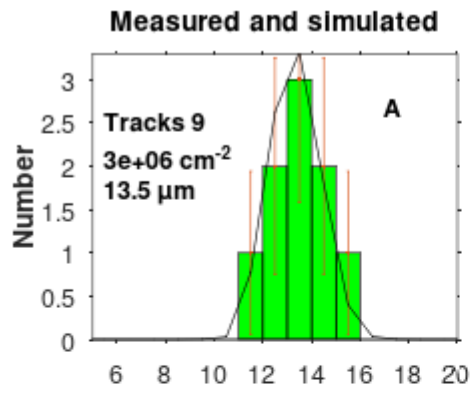


Fig. S8. CXII-06.

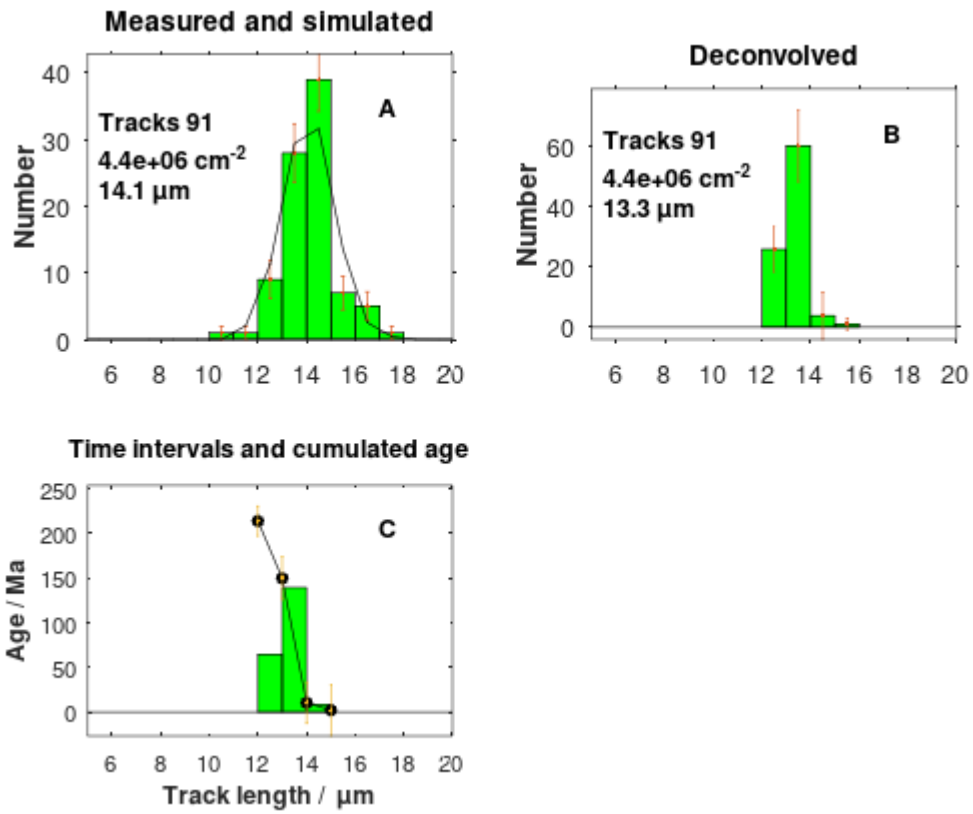


Fig. S9. CXII-13.

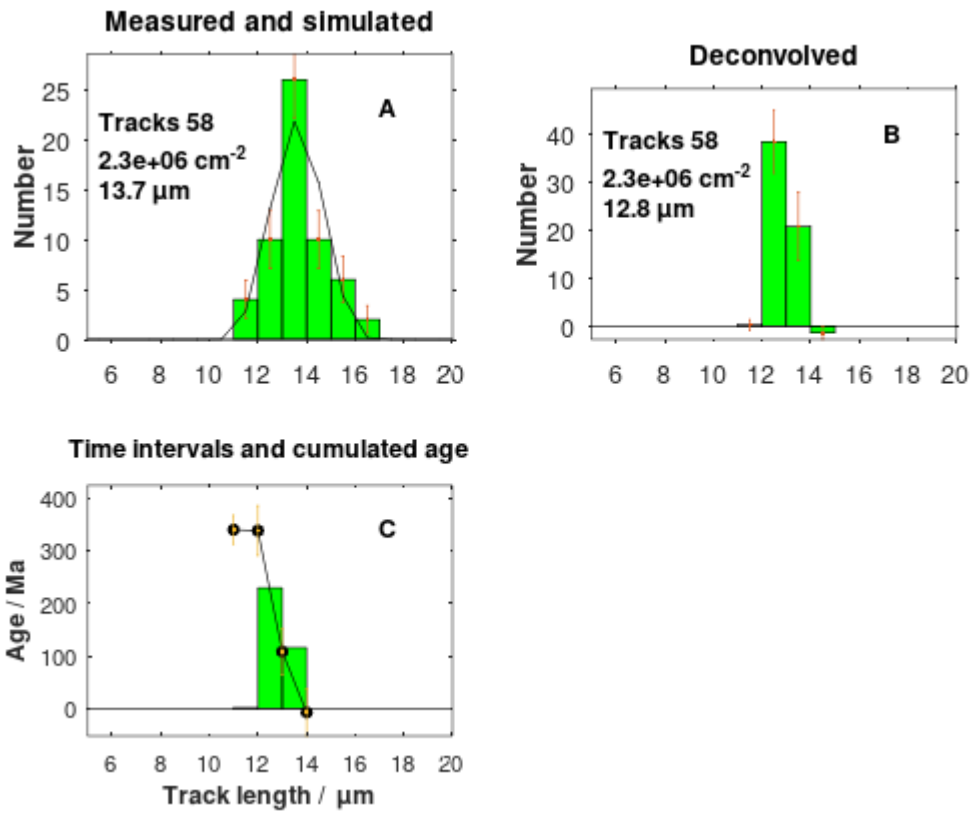


Fig. S10. CXII-14.

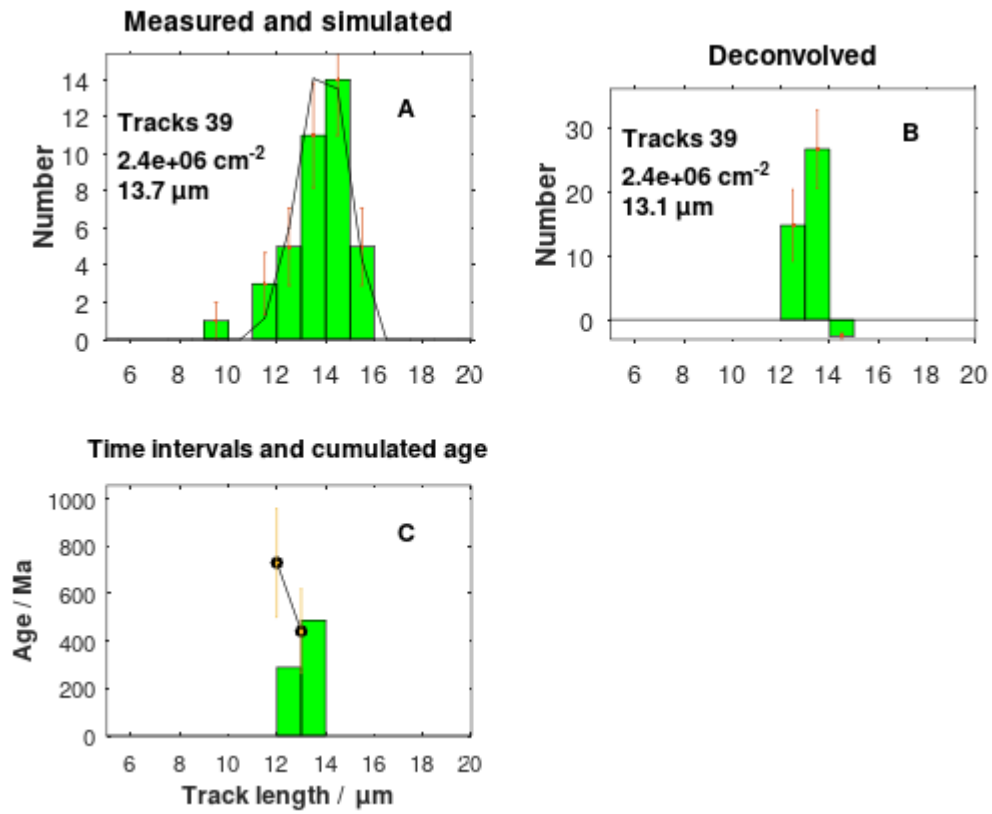


Fig. S11. CXII-20.

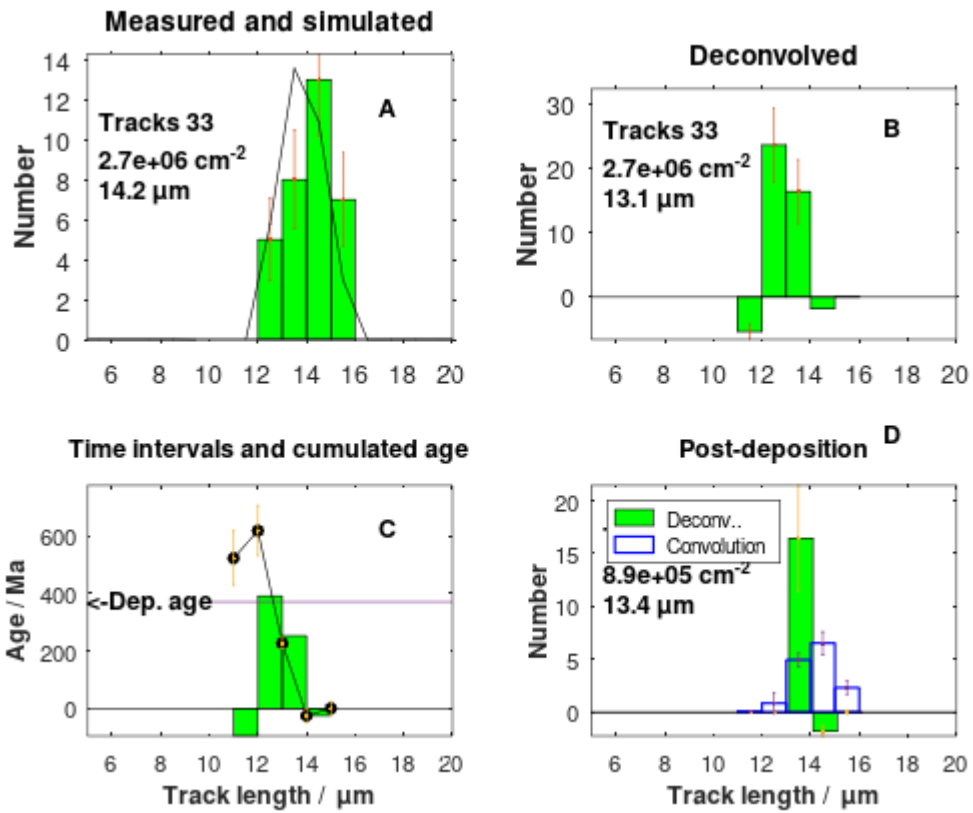


Fig. S12. CXII-22.

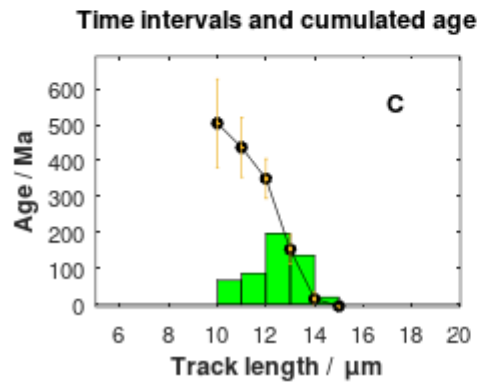
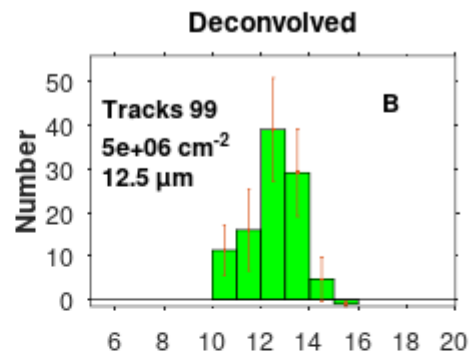
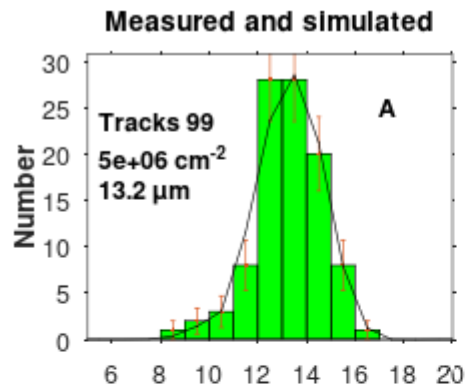


Fig. S13. CXII-25.

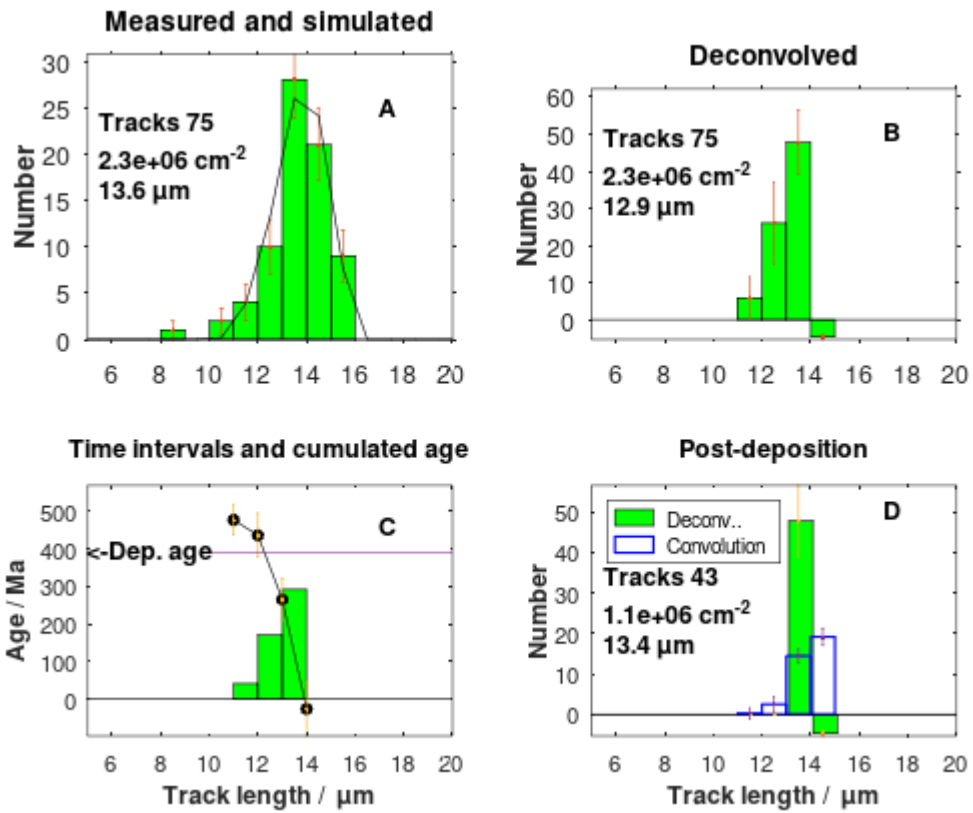


Fig. S14. CXII-27.

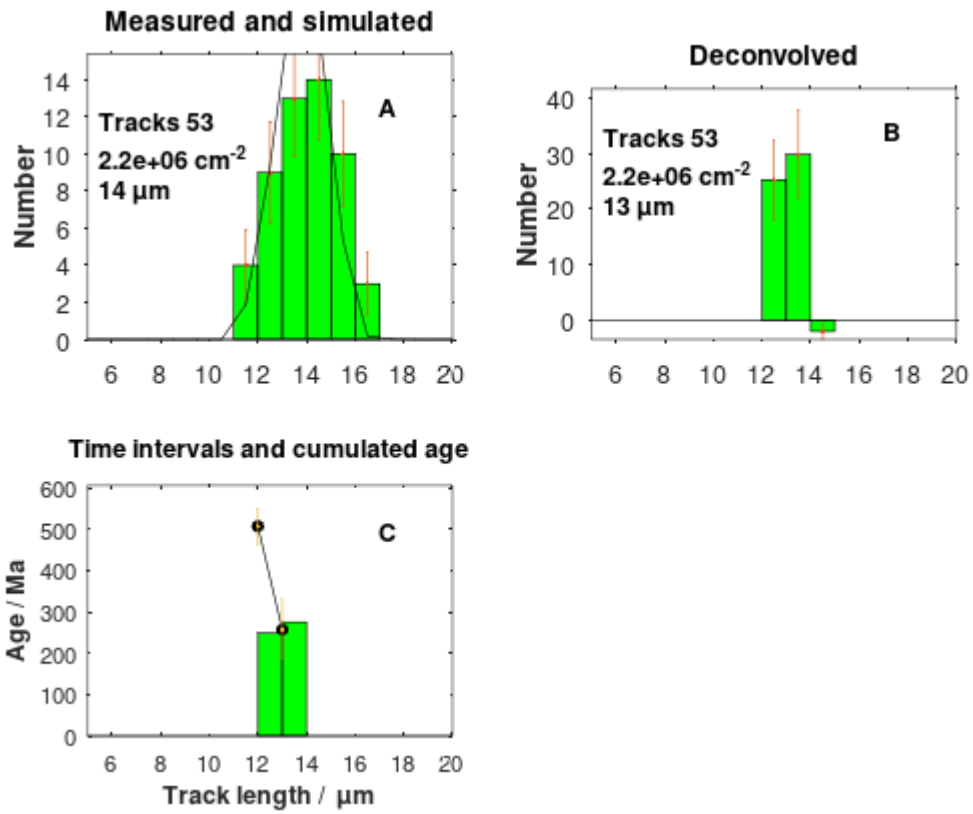


Fig. S15. CXII-30.

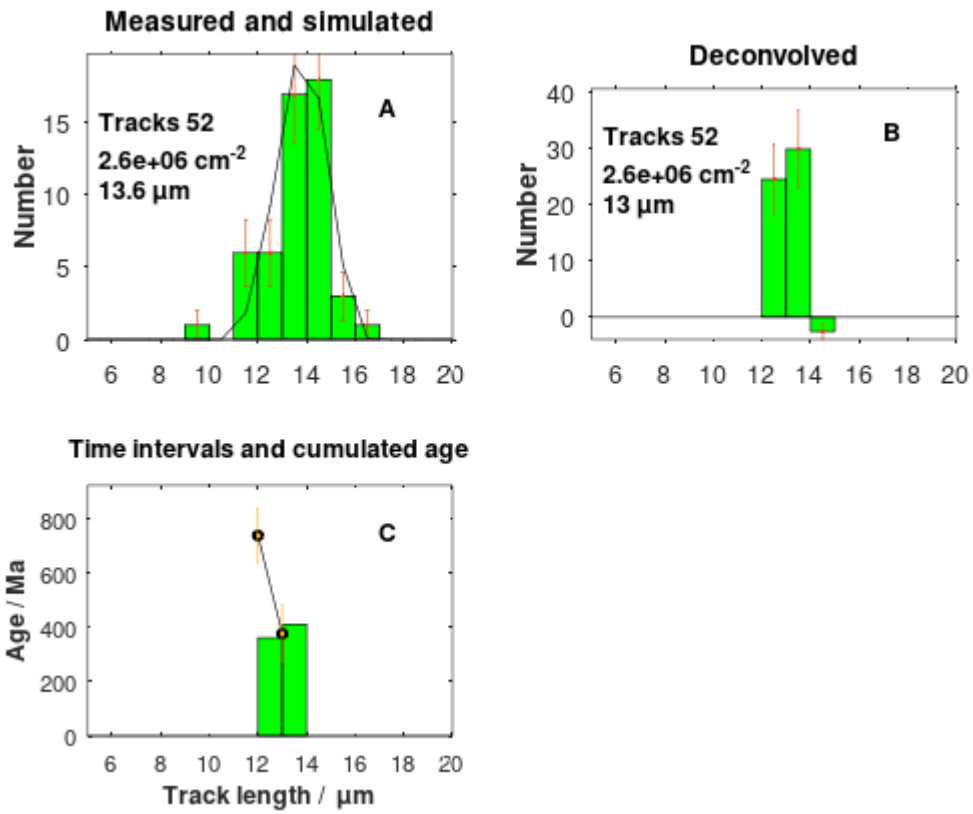


Fig. S16. CXII-36.

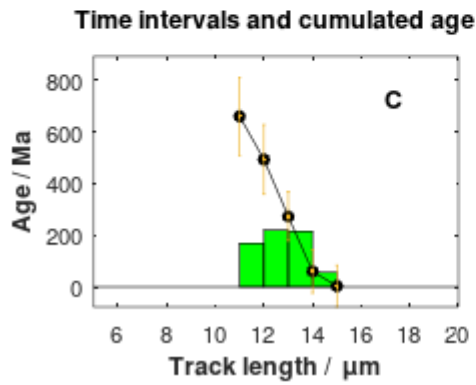
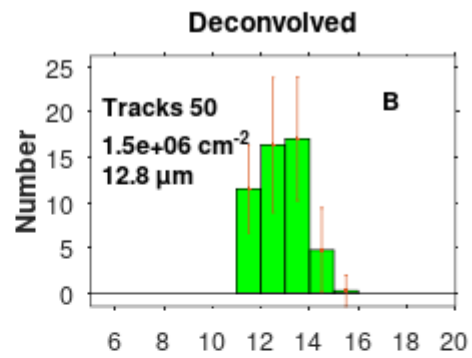
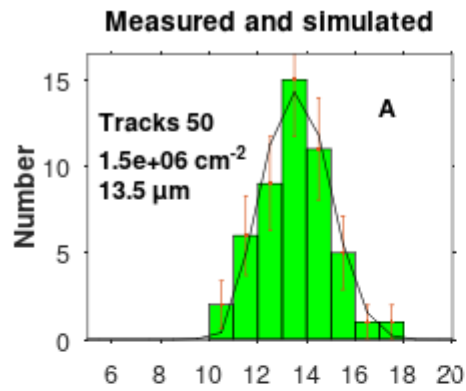


Fig. S17. CXII-37.

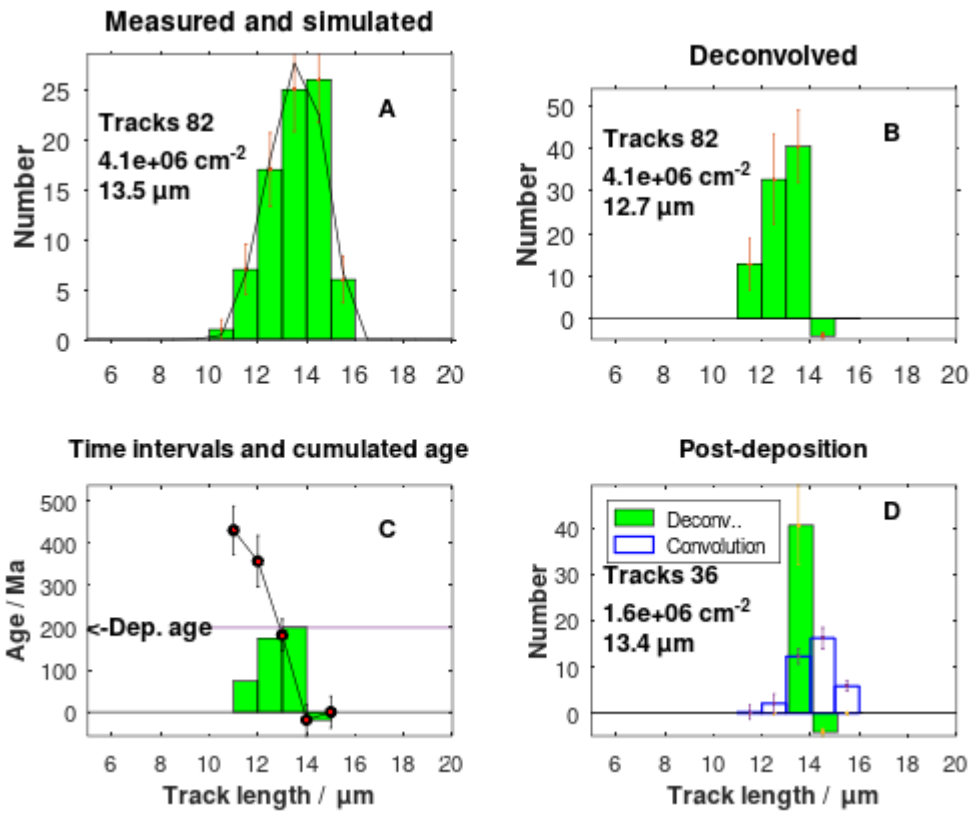


Fig. S18. CXII-42

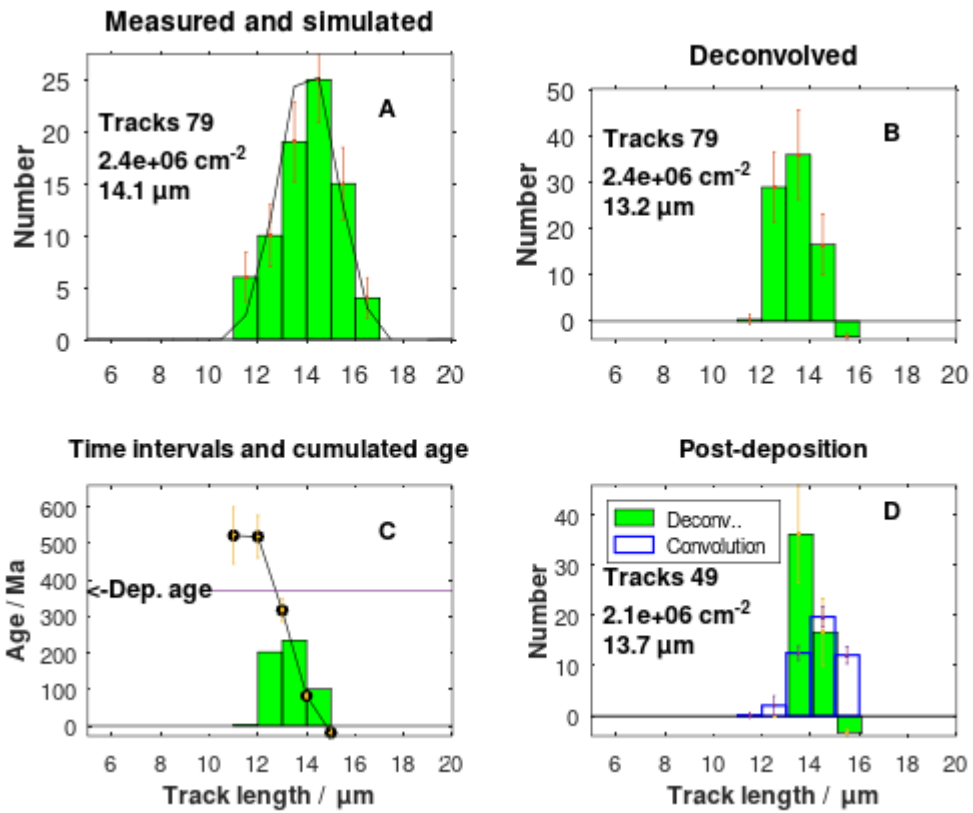


Fig. S19. CXII-46.

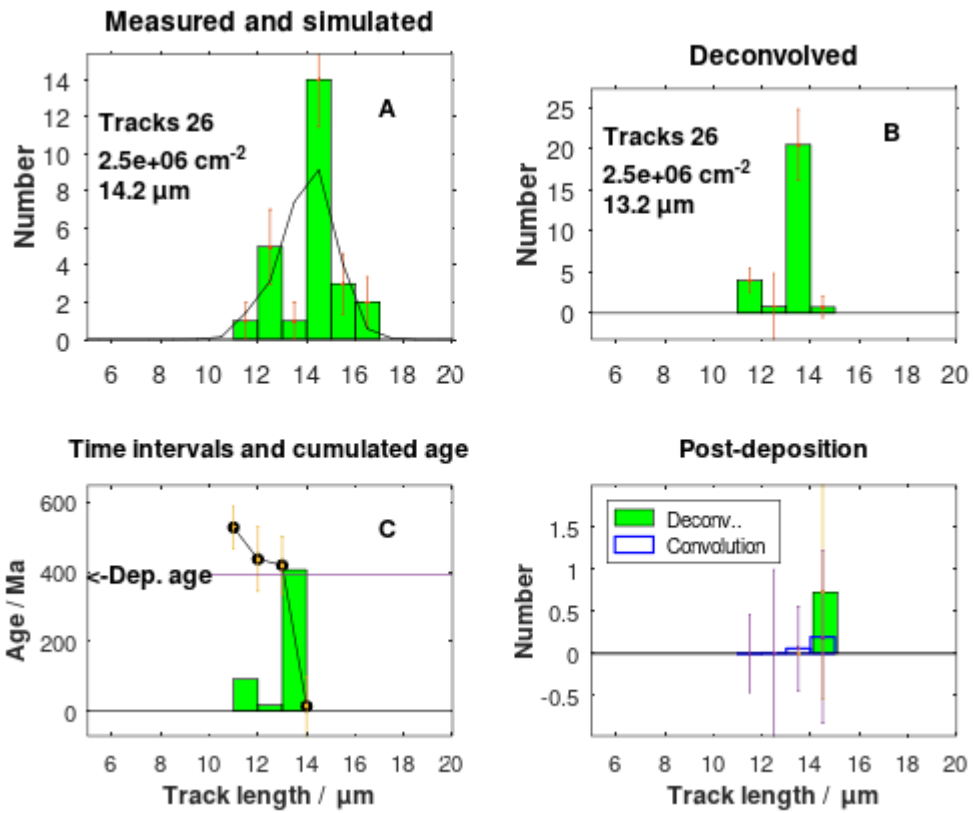


Fig. S20. CXII-48.

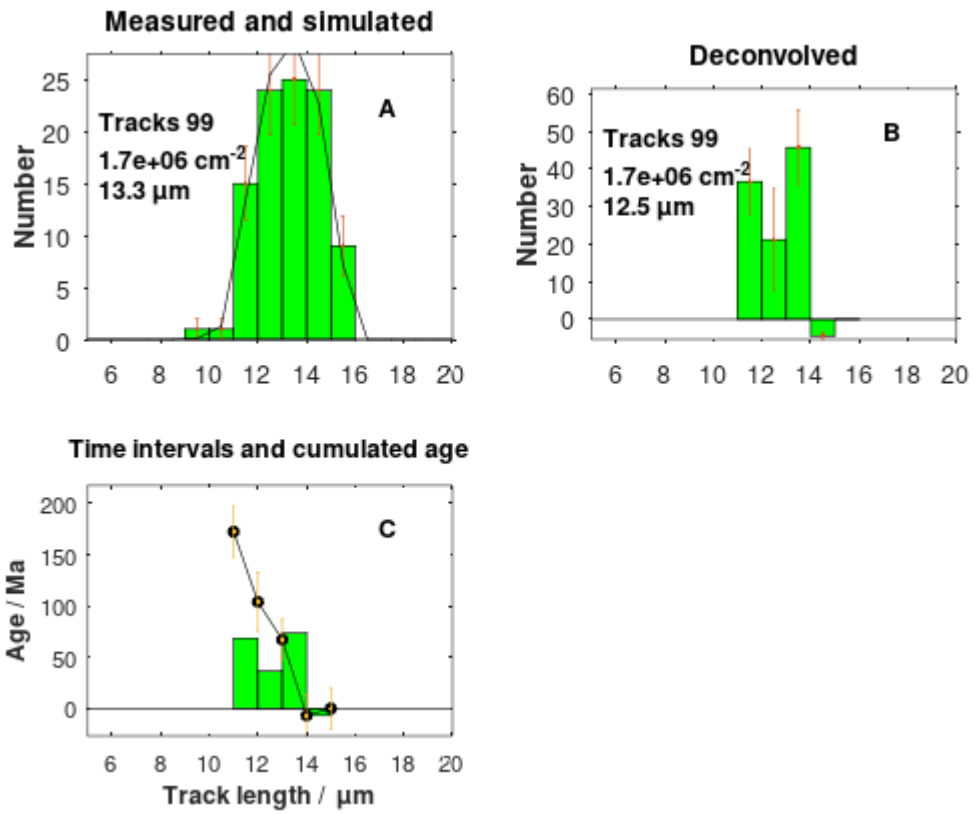


Fig. S21. GRÖ-21.

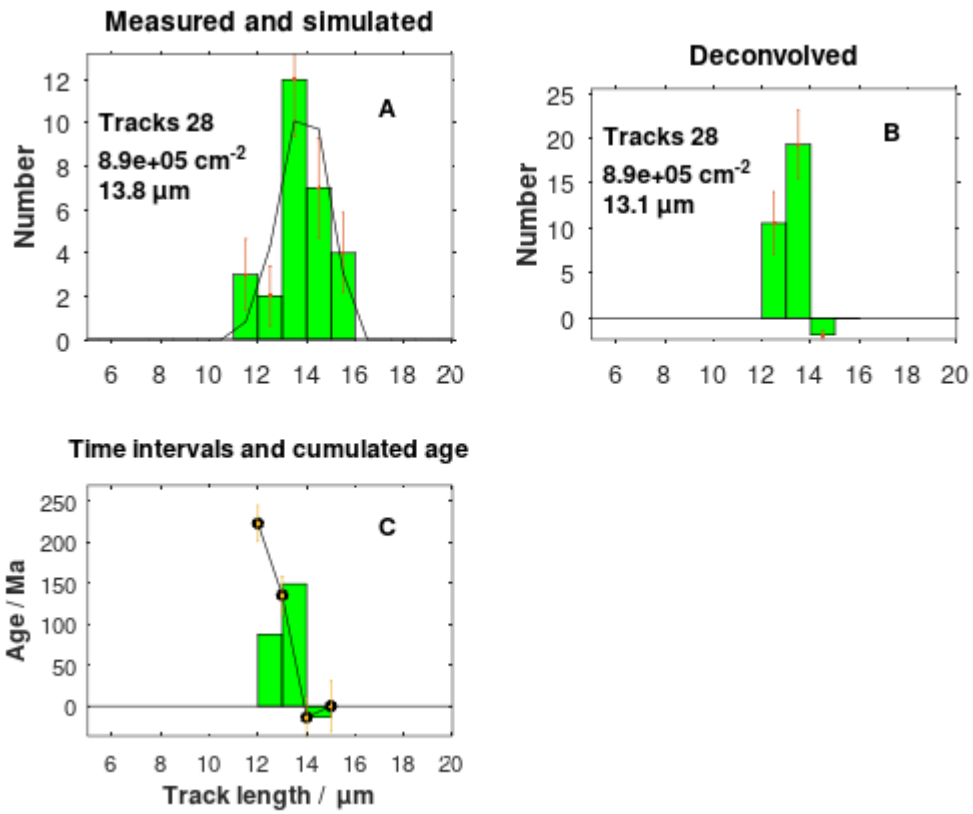


Fig. S22. GRÖ-23.

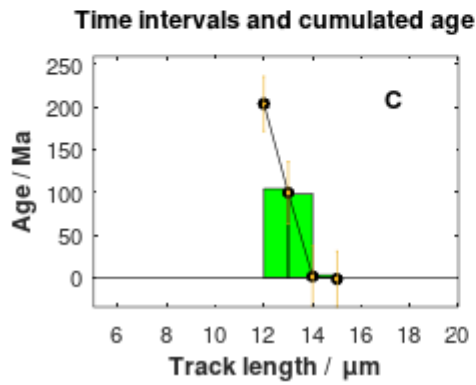
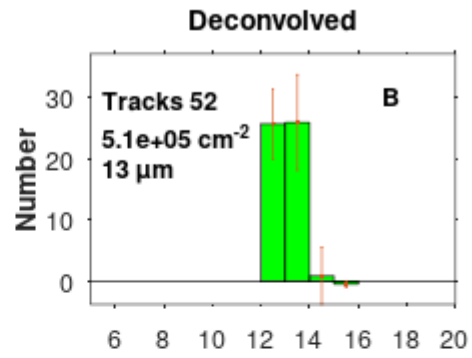
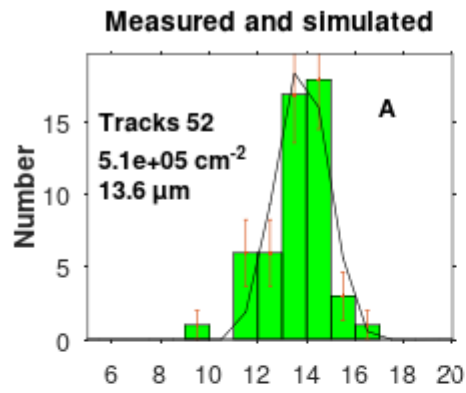


Fig. S23. GRÖ-36.

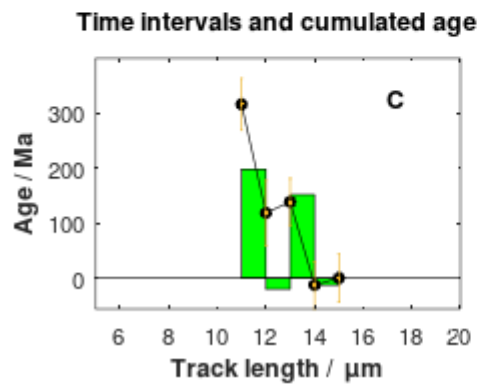
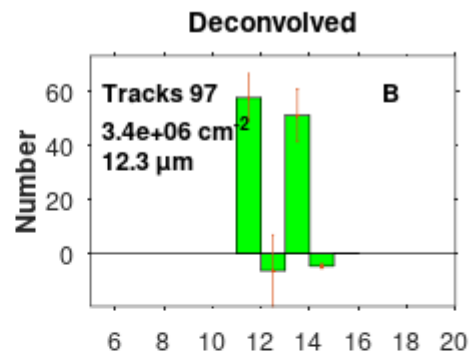
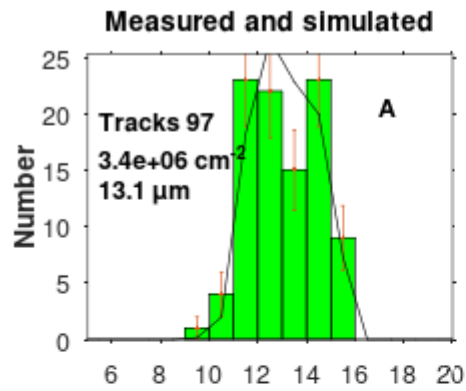


Fig. S24. GRÖ-64.

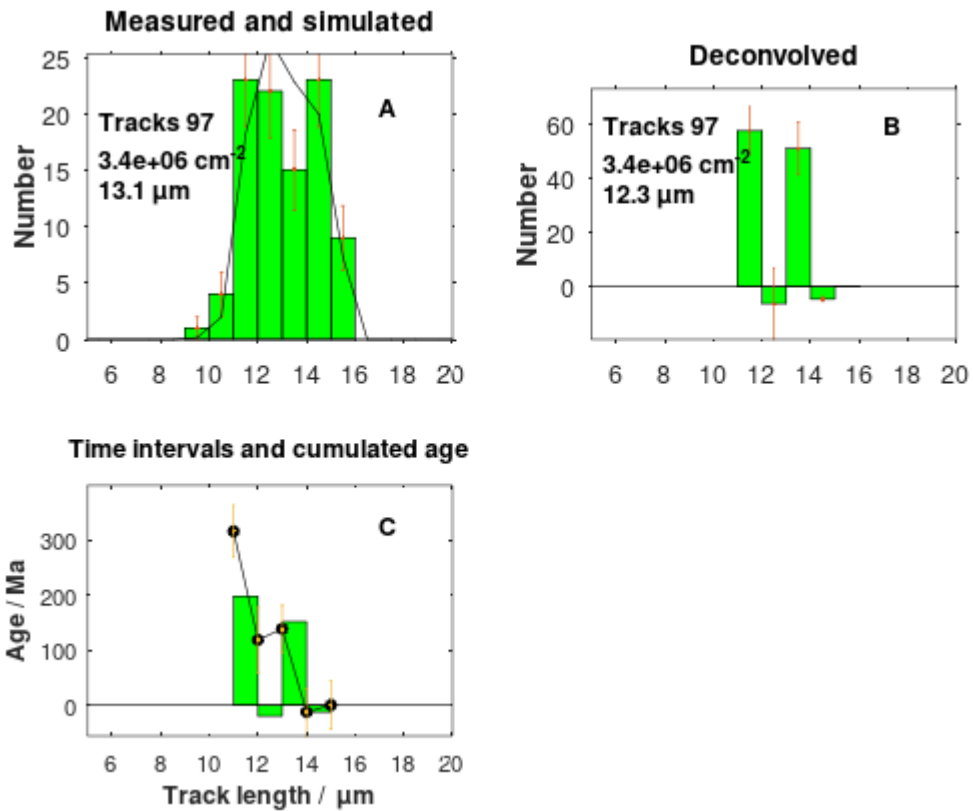


Fig. S25. KP702.

References

Spiegel, C., Sohi, M. S., Reiter, W., Meier, K., Ventura, B., Lisker, F., et al. Phanerozoic tectonic and sedimentation history of the Arctic: Constraints from deep-time low-temperature thermochronology data of Ellesmere Island and Northwest Greenland. *Tectonics*, 42, e2022TC007579. <https://doi.org/10.1029/2022TC007579>, 2023a.

Spiegel, C., Sohi, M. S., Reiter, W., Meier, K., Ventura, B., Lisker, F., et al Supporting Information for Phanerozoic tectonic and sedimentation history of the Arctic: constraints from deep-time low-temperature thermochronology data of Ellesmere Island and Northwest Greenland <https://doi.org/10.5281/zenodo.8120628>, 2023b.